Crystallization Kinetics of Poly(ethylene terephthalate)/Poly(ethylene 2,6-naphthalate) Blends

YU SHI, SALEH A. JABARIN

Polymer Institute, University of Toledo, Toledo, Ohio 43606-3390

ABSTRACT: The crystallization kinetics of poly(ethylene terephthalate)/poly(ethylene 2,6-naphthalate) (PET/PEN) blends were investigated by DSC as functions of crystallization temperature, blend composition, and PET and PEN source. Isothermal crystallization kinetics were evaluated in terms of the Avrami equation. The Avrami exponent (n) is different for PET, PEN, and the blends, indicating different crystallization mechanisms occurring in blends than those in pure PET and PEN. Activation energies of crystallization were calculated from the rate constants, using an Arrhenius-type expression. Regime theory was used to elucidate the crystallization course of PET/PEN blends as well as that of unblended PET and PEN. The transition from regime II to regime III was clearly observed for each blend sample as the crystallization temperature was decreased. © 2001 John Wiley & Sons, Inc. J Appl Polym Sci 81: 23–37, 2001

Key words: PET/PEN blend; crystallization kinetics; Avrami equation; regime theory

INTRODUCTION

The glass-transition temperature and the melting behavior of poly(ethylene terephthalate)/poly(ethylene 2,6-naphthalate) (PET/PEN) blends were discussed in a previous study.[1] This work continues a series of investigations on PET/PEN blends and concentrates on the study of crystallization kinetics.

The crystallization of PET has been investigated for a long time. Cobbs and Burton[2] studied the course of crystallization of PET film with infrared and density measurements. The kinetics of crystallization were analyzed in terms of the Avrami equation. An Avrami exponent (n) was obtained and was interpreted in terms of plate-like growth, as crystallites formed at crystalliza-

tion temperatures between 120 and 180°C. Morgan and coworkers[3,4] compared the crystallization rates of different PET samples with similar molecular weights but polymerized with different polycondensation methods. Jackson and Longman[5] studied the effects of molecular weight, certain catalyst residues, and nucleating agents on the rates of crystallization from the melt of PET and related copolymers. Van Antwerpen and Van Krevelen[6] studied the influence of crystallization temperature, molecular weight, and additives on the spherulite growth rate of PET during crystallization. Gunther and Zachmann[7] investigated the effects of the amounts and kinds of catalyst systems on the half-time of crystallization and orientation of PET. Jabarin[8–10] studied the crystallization behavior of a variety of PET materials. He studied the effects of molecular weight, catalyst system, crystallization temperature, DEG content, and polymerization process on the crystallization of PET. The results were interpreted in terms of the Avrami equation. The Avrami expo-

nent (n) was calculated and the rate constant (k) was investigated.

There are also some reports of crystallization studies of PEN.[11–16] However, there are few reports on the crystallization and melting behavior of the PET and PEN blends.[17–19] Heisey and Hoffmann[17] studied the crystallization behavior of dimethyl 2,6-naphthalene dicarboxylate (NDC)–containing blends and copolymers passed through a Killion extruder. As has been pointed out by some other investigators,[20–26] the degree of randomness or transesterification of a polyester blend affects blend clarity and crystallization behavior. Heisey et al.[17] showed that PEN crystallized at higher temperatures and slower rates than did PET. They also found that the blends crystallized faster than copolymers of the same molar composition. All of the blends that were passed through the extruder three times were clear. Crystallization of blends containing 5 to 15 mol % NDC were not affected by the length of time the blends were melt processed. The study in our laboratory[27] showed similar results. In other words, the transesterification level achieved during melt processing is not a controlling factor for the thermal properties of the blends after a certain transesterification level is achieved and within the transesterification level range investigated in our study. Thus, the blend properties (after a certain transesterification level has been achieved) do not change any more with the transesterification level. This makes it possible to use the blends within the stabilized region, to represent the same composition blend properties.

Lu and Windle[19] studied the crystallization behavior of random copolymers of PEN and PET and found that their crystallinity decreased with NDC content, passed through a minimum at intermediate NDC composition, and increased again with NDC content. In the composition range of 0–60 mol % PET, the X-ray patterns were quite similar to that for the PEN homopolymer, whereas the patterns for the copolymers with 80–100 mol % PET units were generally similar to each other, but distinct from those in the 0–60 mol % PET range. Santa Cruz et al.[24] studied the crystalline structure of random copolymers of PET and PEN and distinguished the regions in which PET or PEN crystallized, while the other component was ejected into the amorphous phase.

Regime theory was proposed by Hoffman et al.[28] for the crystallization kinetics of polymers. They found two straight lines appeared on the plot of log G + $U/2.303R(T - T_0)$ against $1/T(\Delta T)$, suggested by nucleation theory, which reflected the transition from regime I to regime II. Here G is the growth rate, U is a universal constant characteristic of the activation energy of chain motion in the melt, R is the gas constant, T is the crystallization temperature, T_0 is the theoretical temperature at which all motion associated with viscous flow or repetition ceases, and ΔT is the degree of supercooling and equals $T_m^0 - T$, where T_m^0 is the equilibrium melting point. Later, Hoffman[29] proposed regime III theory in polymer crystallization. This theory predicts a twofold increase in the slope of plots of log G + $U/2.303R(T - T_0)$ versus $1/T(\Delta T)$ as the crystallization temperature is lowered through the transition point between regime II and regime III. Three regimes of polymer crystallization have been proposed on both theoretical and experimental grounds. A regime transition occurs when the relationship between growth rate and the surface nucleation rate undergoes a change. In the highest temperature regime (regime I), the observable growth rate varies with i, where i is the surface nucleation rate. In regime II, multiple nucleation occurs on the substrate and G is proportional to $i^{1/2}$, which leads to a downward break in the growth rate curve as it passes through the regime I to regime II transition.[30,31] At still lower temperatures, the mean separation of the nuclei on the substrate approaches the width of the molecular stems, and regime III is observed.[32,33]

PET and PEN form miscible blends within the range of the transesterification levels obtained in our study.[1,27] Results indicated that, after a critical level of transesterification has been reached, thermal properties remained unchanged with additional processing and levels of transesterification. The melting behavior and melting-point depression, resulting from the formation of the miscible blends, were studied in the previous investigation.[1] The crystallization behavior and kinetics of crystallization are expected to be similarly altered by formation of miscible blends of PET and PEN. The crystallization of miscible blends has attracted interest in recent years as an outcome of the study of the miscible blends of crystalline polymers. Mandelkern[34] studied the crystallization kinetics in polymer–diluent mixtures and found that the crystallization behavior for a polymer–diluent mixture is very similar to that for pure polymers. The crystallization kinetics can be interpreted by modifying the method applied to the pure polymer, by assuming that

steady-state nucleation and growth occur simultaneously throughout the process. Hsiao et al.[35] studied the crystallization in miscible poly(aryl ether ketone) (PAEK) and poly(ether imide) (PEI) blends. They observed a transition of regime II to regime III in both pure PAEK and its blends. By using the theory for the polymer–diluent mixtures, they calculated the surface free energy of chain folding.

In this study the crystallization kinetics of PET/PEN blends were investigated as to how they are influenced by crystallization temperature, blend composition, and different PET and PEN materials. The regime theory was used to study the crystallization kinetics of not only pure PET and PEN but also their blends. A differential scanning calorimeter (DSC) was used to investigate the crystallization behavior because it has been shown to be applicable to the study of polymer crystallization.[36–38]

EXPERIMENTAL

Materials

Two PETs and two PENs were used to make the blends. PET 1 is a homopolymer with an intrinsic viscosity (IV) of 0.72, manufactured by Eastman Chemical Co. (Kingsport, TN). PET 2 is an isophthalic acid (IPA)–modified copolymer with an IV of 0.80, manufactured by Shell Chemical Co. (Akron, OH). Both PEN 1 and PEN 2 are homopolymers manufactured by Hoechst (Spartanburg, SC), with IVs of 0.57 and 0.63, respectively. The IV determination of PET was done at 25°C in 60/40 (w/w) phenol/tetrachloroethane solution, whereas the IV of PEN was determined at 30°C in the same solution. Two blend systems were formed by using PET 1 with PEN 1 as blend system A and PET 2 with PEN 2 as blend system B. Blend compositions investigated ranged from 100% PET to 100% PEN.

Previous work[27] showed that after a certain transesterification level has been achieved, thermal properties depend only on blend composition and that the degree of randomness is not a controlling factor. This critical level of transesterification (randomness) that must be reached is generally indicated by optical clarity and a single narrow ΔT_g of about 10°C or less. For these experiments, it was achieved within three passes through the single-screw extruder. Additional passes yielded increased percentage transesteri-

fication; however, no additional changes were noted for optical clarity, the glass-transition temperature, or melting behavior. It should be noted that processing conditions required to attain complete randomization would include longer processing times and/or higher processing temperatures. Either of these conditions could cause severe degradation, which would overcome the transesterification process. The thermal properties, described in the following sections, all represent values obtained after critical transesterification was achieved, as demonstrated by optical clarity and a narrow ΔT_g.[1]

Extrusion

Amorphous films 26–41 mils thick were prepared using a Brabender single-screw extruder with a general-purpose 0.75-in.-diameter screw and length-to-diameter ratio (L/D) of 22 : 1. A screw speed of 80 rpm and extrusion temperature of 300°C were utilized. The polymers were dried at 120°C for 20 h in a Forma Scientific Model 3237 vacuum oven (Marietta, OH) prior to extrusion. The dried polymers were then mixed and extruded. Multiple passes were run to achieve different transesterification levels. Before each extruder pass, the films were chopped, crystallized, and dried at 120°C for 20 h.

Differential Scanning Calorimeter (DSC)

A Perkin–Elmer DSC-2 instrument (Perkin–Elmer, Norwalk, CT) was used. All samples were dried in a vacuum oven at 40°C for 20 h prior to measurements. The calorimeter was operated with a stream of oxygen-free, dry nitrogen flowing over the sample and the reference. During an isothermal scan, the temperature of the sample was increased at 320°C/min to the desired crystallization temperature. The thermal transitions were recorded at this temperature as a function of time. The fractional crystallization as a function of time was then evaluated from the DSC thermogram.

RESULTS AND DISCUSSION

Isothermal Crystallization Kinetics

Experimental Results

In work on polymer crystallization, it is customary to represent the experimental results in terms of the fraction of uncrystallized material,
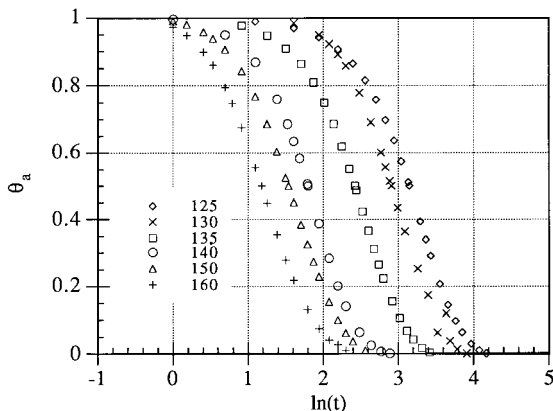
Figure 1 Crystallization isotherms for PET 2 at various crystallization temperatures.

θ_a, as a function of time [$\ln(t)$]. These plots are called crystallization isotherms. For example, the variation of θ_a with time for PET 2 and 40/60 PEN/PET B blend samples, at various crystallization temperatures, is shown in Figures 1 and 2. Similar curves were obtained for all the samples. All of the isotherms have sigmoidal shapes typical of polymer crystallization behavior. In many cases, the curves for different crystallization temperatures may be exactly superposed by shifting horizontally along the axis of $\ln(t)$, indicating that similar crystallization mechanisms are occurring.

Analysis of Results

The crystallization kinetics of polymers are analyzed in terms of the Avrami expression given in eq. (1):
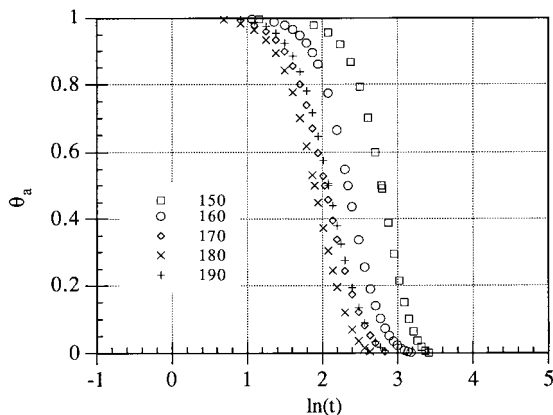
$$\theta_a = \exp(-kt^n) \qquad (1)$$

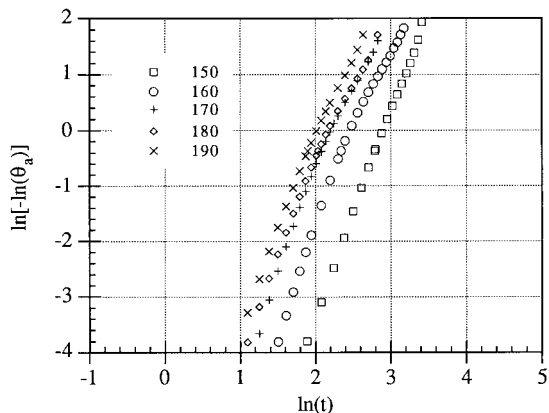**Figure 2** Crystallization isotherms for 40/60 PEN/PET B Blends.

Figure 3 $\ln[-\ln(\theta_a)]$ versus $\ln(t)$ for 40/60 PEN/PET B blends.

where θ_a is the fraction of uncrystallized material, k is the crystallization rate constant, t is the time, and n is the Avrami exponent describing the mechanism of crystallization.

The mathematical formulation of the kinetic phase change and the derivation of the Avrami equation can be found in many sources.[39–41] In the Avrami equation, the kinetic rate constant (k) is a function of the nucleation and the spherulite growth rates. The Avrami exponent provides qualitative information on the nature of nucleation and the growth process.

The kinetic parameters are obtained from eq. (1) by plotting the data according to eq. (2):

$$\ln[-\ln(\theta_a)] = \ln(k) + n \ln(t) \qquad (2)$$

Therefore, a plot of $\ln[-\ln(\theta_a)]$ versus $\ln(t)$ yields a straight line, the slope of the primary or initial crystallization portion is equal to n, and the intercept is equal to $\ln(k)$.

A typical example of Avrami plots for the crystallization behavior of one composition blend, 40/60 PEN/PET B blend sample, is shown in Figure 3. Similar plots were constructed for all the blend samples as well as for pure PET and PEN. Summaries of n values and the rate constants for the crystallization behaviors of the various blend samples are given in Tables I and II. Compositions are given as PEN/PET (w/w) blending ratios, as well as mol % dimethyl-2,6-naphthalene dicarboxylate (NDC) composition, measured with NMR as described in our study concerning the transesterification reaction kinetics of the blends.[42]
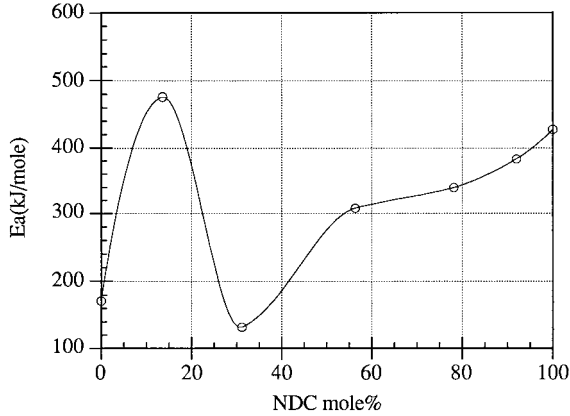
Table I Avrami Exponent n and Rate Constant (k) Values for A Blend Samples

	PET 1		PEN/PET A Blends (w/w Composition)								PEN 1	
Composition	0/100		20/80		40/60		60/40		80/20		100/0	
NDC (mol %)	0		13.56		31.18		56.34		78.15		100	
T_c (°C)	k (s^{-n})	n	k (s^{-n})	n	k (s^{-n})	n	k (s^{-n})	n	k (s^{-n})	n	k (s^{-n})	n
120	1.12×10^{-5}	2.7	5.40×10^{-6}	—								
125	7.31×10^{-5}	2.7										
130			4.47×10^{-4}	3.9								
140	3.08×10^{-4}	2.9	6.28×10^{-3}	3.9	—	4.0						
150	4.78×10^{-3}	2.8					1.17×10^{-6}	3.9	2.92×10^{-6}	3.8		
160	6.57×10^{-3}	—			1.22×10^{-4}	4.0	1.04×10^{-4}	—	5.31×10^{-4}	—		
170					1.99×10^{-4}	4.0	1.99×10^{-4}	3.8	3.60×10^{-4}	4.0	3.67×10^{-7}	3.7
180					6.19×10^{-4}	3.8	5.59×10^{-4}	3.6	5.88×10^{-3}	3.9	4.72×10^{-6}	4.0
190					2.62×10^{-4}	3.9	—	3.9	7.31×10^{-3}	3.2	6.77×10^{-5}	3.3
200									—	3.9	5.36×10^{-4}	3.4

Table II Avrami Exponent n and Rate Constant (k) Values for B Blend Samples

	PET 2		PEN/PET B Blends (w/w Composition)										PEN 2	
Composition	0/100		5/95		10/90		20/80		40/60		60/40		100/0	
NDC (mol %)	0		3.56		7.55		17.66		33.26		53.88		100	
T_c (°C)	k (s^{-n})	n	k (s^{-n})	n	k (s^{-n})	n	k (s^{-n})	n	k (s^{-n})	n	k (s^{-n})	n	k (s^{-n})	n
105	1.61×10^{-5}	—	1.55×10^{-6}	4.0										
110	1.72×10^{-5}	—	1.71×10^{-5}	4.0										
113			7.51×10^{-5}	4.0	2.17×10^{-7}	4.0								
115		3.0			9.45×10^{-6}	4.0	9.20×10^{-8}	4.0						
120		4.0			1.76×10^{-4}	4.0	1.53×10^{-6}	4.0						
125							1.61×10^{-5}	4.0						
130	1.41×10^{-4}	3.0												
140									4.10×10^{-7}	4.0	6.00×10^{-9}	4.0		
150		2.9							1.58×10^{-5}	4.0	4.76×10^{-7}	4.0		
160									5.93×10^{-5}	4.0	1.80×10^{-5}	4.0	1.62×10^{-6}	3.0
170											1.39×10^{-4}	—	4.94×10^{-5}	3.0
190													3.28×10^{-3}	3.1
210													7.35×10^{-3}	3.1

Figure 4 Activation energy versus NDC content for A blends.

The Arrhenius equation can be used to illustrate the temperature dependence of the rate constant (k), that is,

$$k = A \exp(-E_a/RT) \qquad (3)$$

where E_a is the apparent activation energy of rate constant (k), A is the frequency factor, T is the crystallization temperature, and R is the gas constant.

From eq. (3), a plot of $\ln(k)$ versus $1/T$ should give a straight line:

$$\ln(k) = \ln(A) - E_a/RT \qquad (4)$$

E_a can be calculated from the slope of this straight line. Using this method, E_a values were calculated for both A and B blend samples and were plotted against blend composition (NDC content), as shown in Figures 4 and 5.

Discussion and Interpretations

Tables I and II give the n values for all the blend samples. It is seen that n is 4 for all the blend samples, whereas n is 3 for pure PET. For pure PEN, n is 3 or 4, depending on the different materials used. The Avrami exponent describes different primary nucleation mechanisms. When n is 4, this means the crystallization mechanism is spherulite growth from sporadic (homogeneous) nucleation. If n equals 3, this indicates a mechanism of spherulite growth from instantaneous (heterogeneous) nucleation. Thus different n values for pure PET, PEN, and blends indicate different crystallization mechanisms.

The rate constant k determines the rate of nucleation and the growth process, which controls crystallization and is extremely sensitive to temperature. A change of 10^3 is observed for a change of crystallization temperature of 30°C. A similar changing trend of the k values for pure PET was observed by Jabarin.[8–10] E_a reflects the temperature sensitivity of the rate constant k. Figures 4 and 5 show E_a as a function of NDC content. For both A and B blends, E_a goes through a minimum for the blends at the intermediate blend composition (NDC content around 33 mol %). In the case of B blends, E_a increases to a very high value if a small amount of either PEN or PET is added to PET or PEN. For A blends, the changing trend from unblended PET to PET-rich blends is the same. From unblended PEN to the blends, however, instead of an increase by adding PET into PEN, E_a decreases as PET content increases. This phenomenon can be explained by the following analysis.

As already known, the rate constant k contains two factors, the nucleation rate and the spherulite growth rate. The relationship can be described in eq. (5)[43] as

$$k = k_0 \exp\left(-\frac{E_d}{RT} - \frac{\Delta G}{RT}\right) \qquad (5)$$

where ΔG is the activation energy necessary to form a nucleus of critical size and E_d is the activation energy of chain jumping or movement, which is sometimes considered to be constant.[21] Heterogeneous (instantaneous) nucleation and homogeneous (sporadic) nucleation give different activation energy (ΔG) values. The heteroge-
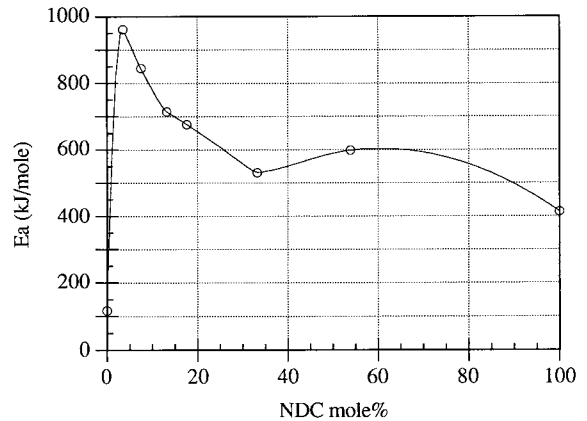

Figure 5 Activation energy versus NDC content for B blends.

neous nucleation is much easier to achieve than is the homogeneous nucleation, because for homogeneous nucleation a higher energy barrier must be crossed for a critical-sized nucleus to form. For heterogeneous nucleation, the nuclei already exist and thus no such energy barrier must be overcome. Therefore, from eq. (5), ΔG for heterogeneous nucleation is much smaller than that for homogeneous nucleation, whereas the spherulite growth rate is similar for both cases.[43] Thus for n equals 4, the activation energy is much higher than that when n equals 3. This explains the increase of E_a from PET to the blends for both blend systems, where n is 3 for both PET materials and n is 4 for all blends. The increase of E_a from that of the unblended PEN value to the blends for the B blend system is explained similarly, where n is 3 for PEN 2 and n is 4 for all blends. No increase in E_a is observed with the addition of PET to PEN 1 because n of PEN 1 is 4, as it is for A system blends.

The plots of E_a versus composition resemble previously obtained plots of blend melting points versus composition.[27] Equilibrium melting point minima were found to occur at intermediate blend compositions and were attributed to the disruption of the crystalline structures by the addition of comonomers. The melting-point depression was also discussed. This disruption reaches its maximum effect when the naphthalate and terephthalate units are more or less equal (NDC content around 33 mol %). In this composition range, the crystalline structures formed are the least perfect and most easily destroyed. The energy barrier for a structure to be destroyed is lower for an imperfect crystalline structure than that for a more perfect one. As was discussed previously, E_a is an energy barrier. From the chemical reaction theory,[44] E_a is equal in both directions (formation or destruction). A lower E_a value in the direction of destruction also indicates a lower E_a value in the direction of formation. An imperfect crystalline structure is therefore more easily destroyed or formed. Thus we expect E_a will assume a minimum value at the least-perfect crystalline structure, as observed from our experimental data shown in Figures 4 and 5. As the crystalline structure becomes more perfect, with an increase in either PET or PEN content, E_a increases. The decrease of E_a from that of unblended PEN by addition of PET for A blends can be explained similarly. For the A blend, PEN 1 was used to make the blends. Table I shows the Avrami exponent n is 4 for both PEN 1 and the various blend compositions for the temperature range in which E_a was calculated. The nucleation mechanism for PEN 1 and its blends is the same. E_a therefore should be in the same range for both pure PEN and its blends. In the meantime, the addition of PET to PEN disrupts the crystal structure of PEN and causes formation of less-perfect crystals. This, in turn, causes the decrease of E_a from pure PEN by the addition of PET.

The changing trend of the activation energy can be elucidated more clearly by regime theory.[28–30,45–48] According to this theory, the spherulite growth rate G is given by[28–30]

$$G = G_0 \exp\left(\frac{-U^*}{R(T_c - T_0)}\right) \exp\left(\frac{-K_g}{T_c \Delta T}\right) \quad (6)$$

where G_0 is a preexponential term; U^* is the activation energy of the elementary jump process commonly assumed to have a universal value of 6276 J/mol[49]; T_c is the crystallization temperature; T_0 is the temperature at which the mobility of the molecules converges to zero and is frequently assumed to be $T_g - 30°$[49]; R is the gas constant; K_g is the nucleation exponent; and ΔT is the degree of supercooling and equals $T_m^0 - T_c$, where T_m^0 is the equilibrium melting point.

The distinction between the three regimes in polymer crystallization is a function of the degree of supercooling and depends on the relationship between the nucleation rate (i) and the overall observable growth rate (G) at various temperatures.[29,48] In regime I, the nucleation rate is much slower; thus, a layer of thickness b_0 and length L is completed before a new nucleation act occurs. As a result, the growth surface of the crystal is essentially smooth for a distance comparable to L, because the new substrate layer is complete before a new nucleus forms. Thus, in regime I, $G(\mathrm{I}) = ib_0L$, which leads to[28,29]

$$K_g(\mathrm{I}) = 4b_0 \sigma \sigma_e \frac{T_m^0}{\Delta Hk} \quad (7)$$

where σ is the lateral surface free energy, σ_e, is the fold surface free energy, ΔH is the enthalpy of fusion, k is Boltzmann's constant, and b_0 is the layer thickness that has been completed. Regime II starts when the nucleation rate increases and multiple nuclei form on the substrate before the previous layer has been completed. On a molecular scale, the newly formed surface in regime II is uneven and rough. The growth rate for regime II
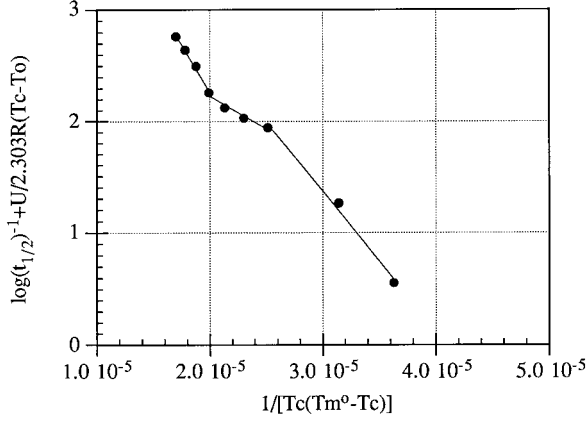
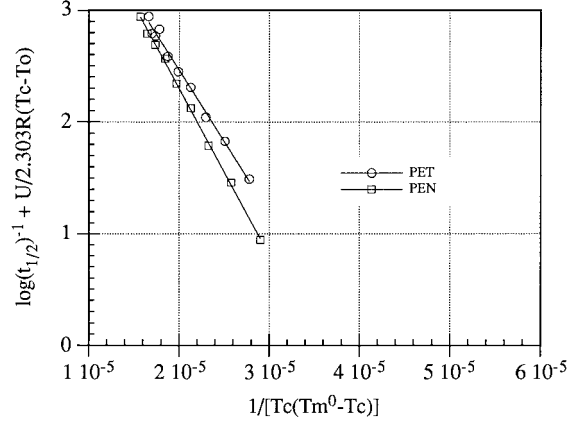**Figure 6**   Plot of eq. (12) for PET 1.

Figure 8   Plot of eq. (12) for PET 2 and PEN 2.

is given by $G(\text{II}) = b_0(2ig)^{1/2}$,[28,29] where g is the rate of the chain folding on the subsurface, and

$$K_g(\text{II}) = 2b_0\sigma\sigma_e\frac{T_m^0}{\Delta Hk} \qquad (8)$$

Regime III crystallization begins when the nucleation rate is so fast that the distance between nuclei is comparable to the width of chain stems. The growth front in regime III is extremely rough.[50] The growth rate is proportional to i, so $G(\text{III}) = b_0 iL$.

$$K_g(\text{III}) = 4b_0\sigma\sigma_e\frac{T_m^0}{\Delta Hk} \qquad (9)$$

For bulk crystallization kinetics, secondary nucleation theory can be applied while assuming[49]

$$k = \frac{4}{3}\pi G^3 N \qquad (10)$$

where N is the number of nucleation sites, which is essentially constant for instantaneous nucleation. In addition, k can also be calculated from the half-time of crystallization $t_{1/2}$.[49,51]

$$k = \ln 2\left(\frac{1}{t_{1/2}}\right)^n \qquad (11)$$

Combining the preceding equations, we obtain

$$\log(t_{1/2})^{-1} + \frac{U}{2.303R(T_c - T_0)}$$

$$= A_2 - \frac{K_g}{2.303T_c(\Delta T)^m} \qquad (12)$$
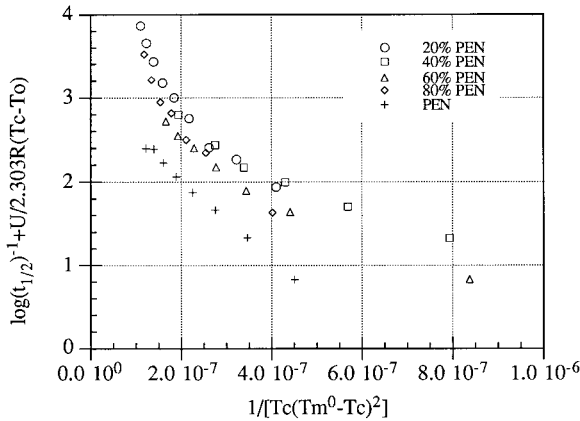
Figure 7   Plot of eq. (12) for PEN 1 and A blends.
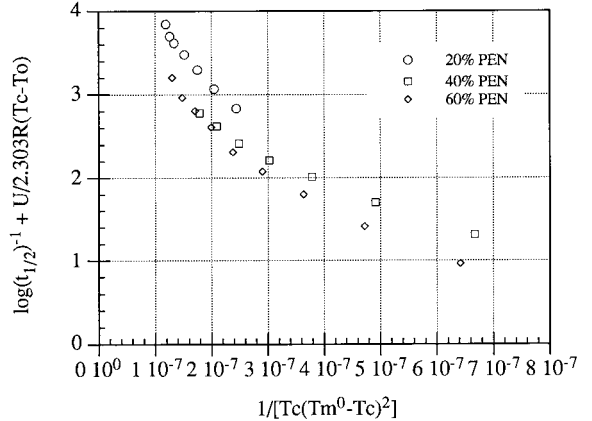
Figure 9   Plot of eq. (12) for B blends.

Table III   Regime Constants for A Blend Samples

NDC (mol %)	Slope 1 ($\times 10^{-5}$)	K_g (II) ($\times 10^{-6}$)	Slope 2 ($\times 10^{-6}$)	K_g(III) ($\times 10^{-6}$)	Ratio K_g(III)/K_g(II)	Transition Temperature (°C)	Supercooling (°C)
0	0.60	0.14	0.15	0.34	2.5	155	121
13.6	39.4	9.07	9.36	21.6	2.4	170	102
31.2	18.6	4.28	4.35	10.0	2.3	170	81
56.3	21.3	4.91	4.78	11.0	2.2	185	84
78.2	46.0	10.6	11.5	26.6	2.5	185	106
100	48.8	11.2	—	—	—	—	—

Thus, the plot of the left-hand side of eq. (12) versus $1/T_c(\Delta T)^m$ will give a straight line, where $m = 1$ for the instantaneous nucleation type and $m = 2$ for the sporadic nucleation type. The construction of the straight line also serves as a test for the regime theory.

Tables I and II show the Avrami exponent (n) for the two blend system samples. Consequently, a different m is used to construct the plot according to eq. (12). The left-hand side of eq. (12) was plotted against $1/T_c(\Delta T)^m$. The resultant plots are shown in Figures 6 and 7 for A blend samples as well as for PET 1 and PEN 1 samples. Here n is 3 for PET samples and n is 4 for PEN 1 and all blend samples. Thus m is 2 for blends and PEN 1 and m is 1 for PET 1. For B blend samples, n is 3 for both PET 2 and PEN 2, whereas n is 4 for all blend samples. Thus m is 2 for all the blends, and m is 1 for PET 2 and PEN 2 for the B blend system. Thus-constructed plots for the B blend system are shown in Figures 8 and 9. To construct eq. (12), the equilibrium melting point for each blend was used and the values were obtained as described in the previous study.[1] Glass-transition temperature (T_g) values were also obtained from the DSC measurement as described in the previous study.[1]

In the cases of both blend systems, the regime transitions can be clearly seen. Regime II and regime III transitions are very clear for all the blend samples, although they are not very clear for both PEN 2 and PET 2. The reason for this might be that the temperature range used for isothermal crystallization of pure PET and PEN is in the lower temperature range and thus the whole regime range was not achieved. The regime transition is also not observed for PEN 1, the reason for which could be the same. For PET 1, however, it seems the whole regime transition range was observed (regimes I–II–III). The reason is that the temperature range used here covers the whole transition range. Thus, different grades of PET appear to have different ranges of transition temperatures. This seems to be related to different copolymers incorporated into PET during polymerization and different polymerization catalyst systems.

The slope of each line was calculated and values of K_g in regimes II and III were obtained for each set. The calculated slope and K_g values are listed in Tables III and IV. The ratios of K_g(III)/K_g(II) are also listed in the same tables. The ratio of K_g(III)/K_g(II) is close to 2 for every blend sam-

Table IV   Regime Constants for B Blend Samples

NDC (mol %)	Slope 1 ($\times 10^{-5}$)	K_g(II) ($\times 10^{-6}$)	Slope 2 ($\times 10^{-6}$)	K_g(III) ($\times 10^{-6}$)	Ratio K_g(III)/K_g(II)	Transition Temperature (°C)	Supercooling (°C)
0	1.27	0.29	—	—	—	—	—
17.7	70.4	16.2	15.2	35.0	2.2	135	131
33.3	24.2	5.57	4.58	10.5	1.9	175	81
53.9	31.6	7.28	6.87	15.8	2.2	180	96
100	1.48	0.34	—	—	—	—	—

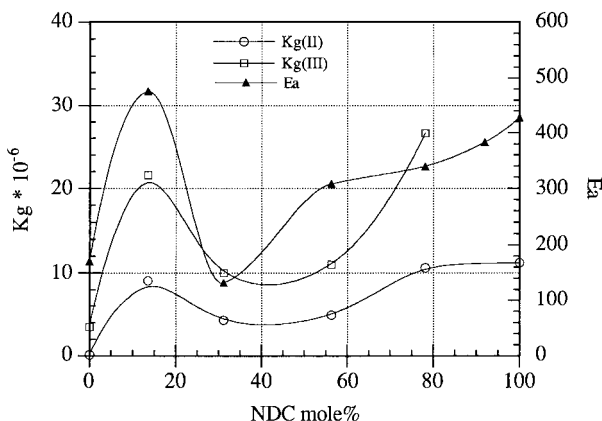**Figure 10** K_g versus NDC content for A blends.

ple, which is the value predicted by the regime theory.

$K_g(II)$ and $K_g(III)$ values were plotted versus blend composition (NDC content) as shown in Figures 10 and 11 for both blend samples. Also shown on the same plot is the curve of activation energy as a function of NDC content. These plots are in agreement with the activation energy plots in Figures 4 and 5. Both the K_g and the activation energy values follow a similar changing trend with NDC content. In both A and B blend systems, the changing trend of $K_g(II)$ is the same as that of the activation energy, when plotted as a function of NDC content. In the case of $K_g(III)$ values, it is not clear because these values were not obtained for unblended PET and PEN. For blend samples, however, the $K_g(III)$ and activation energy curves follow the same kind of curve. They all show a minimum at the intermediate concentration, indicating smaller surface free energy for the formation of less-perfect crystalline structures at this intermediate composition range. The reason for the K_g value increase from both the PET and PEN sides for the B blends is the same as given previously to explain the changes in activation energy. This is also in agreement with the Avrami exponent values measured for these samples. The increase of K_g is the result of the homogeneous nucleation versus the heterogeneous nucleation. Heterogeneous nucleation results in much lower K_g values than does homogeneous nucleation. The free energy for the formation of the nucleation is thus much lower for the heterogeneous nucleation than that for the homogeneous nucleation. This accounts for the observation of the increase in E_a. In the case of the blends, K_g goes through a minimum as E_a

does, which indicates lower K_g values at these intermediate composition ranges. The nuclei in this range are most easily formed because of the extremely rough surface of chain folding. Thus the K_g value is smallest in this composition range. The difference in the absolute values for the K_g from the PET side and the PEN side might result from the formation of different crystal structures in PET-rich blends than in the PEN-rich blends.

The temperatures of the transitions from regime II to regime III are shown in Tables III and IV. Using the equilibrium melting points calculated in the previous study,[1] the degree of supercooling was calculated for the transition point from regime II to regime III. The calculated degree of supercooling is also listed in Tables III and IV. It is noteworthy that the degree of supercooling for the regime transition to occur is different for blend samples with different compositions. The degree of supercooling required for the transition to occur also changes in a manner similar to that of both K_g and the activation energy. This means that the topography of the crystalline phase formed in the blend is different from that of pure PET and PEN.

Hsiao et al.[35] studied the crystallization of miscible blends of PAEK/PEI, where they considered the diluent effect of the noncrystallizable component and accordingly adjusted the free energy of nucleation (i.e., K_g term). In our previous discussion, we considered that the effect of the noncrystalline component was incorporated in the equilibrium melting points and the modified glass-transition temperatures. Thus, additional modification in the K_g term in eq. (12) was not accommodated.

According to eqs. (7) to (9), the surface free energy can be calculated from the slope value of
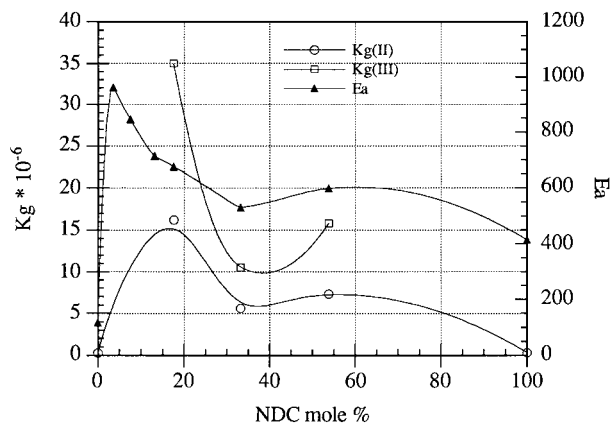

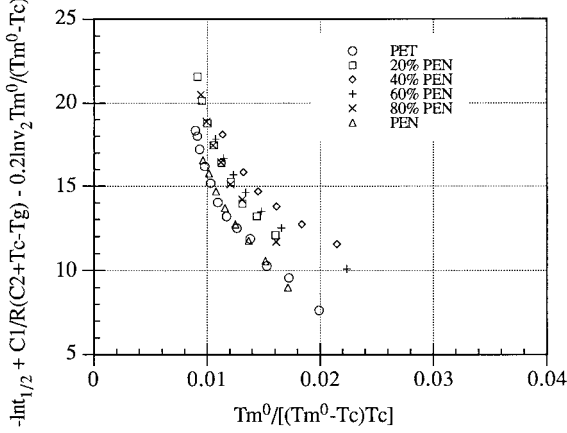**Figure 11** K_g versus NDC content for B blends.

Figure 12   Plot of eq. (19) for A blends.

$$- C_1/[R(C_2 + T - T_g)]$$

where C_1 is 4120 cal/mol and C_2 is 51.6°. Substituting this term into eq. (6) and combining with eq. (13), we obtain eq (15):

$$G = G_0 \exp\left(\frac{- C_1}{R(C_2 + T - T_g)}\right)$$
$$\exp\left(\frac{- 4b_0\sigma\sigma_e T_m}{k\Delta H(T_m - T)T}\right)\exp\left(\frac{2\sigma \ln \varphi_2 T_m}{b_0\Delta H(T_m - T)}\right) \quad (15)$$

To simplify eq. (15) an empirical relation $\sigma = 0.1b_0\Delta H$[53] was used here. Thus,

$$G = G_0 \exp\left(\frac{- C_1}{R(C_2 + T - T_g)}\right)$$
$$\exp\left(\frac{- 4b_0\sigma\sigma_e T_m}{k\Delta H(T_m - T)T}\right)\exp\left(\frac{0.2 \ln \varphi_2 T_m}{T_m - T}\right) \quad (16)$$

Now we will make another assumption. We assume that a half-time value can be used to represent the bulk growth rate, which is proportional to the linear growth rate. The following equations can then be obtained:

Regimes I and III

$$-\ln t_{1/2} + \frac{C_1}{R(C_2 + T - T_g)} - 0.2 \ln \varphi_2\frac{T_m}{T_m - T}$$
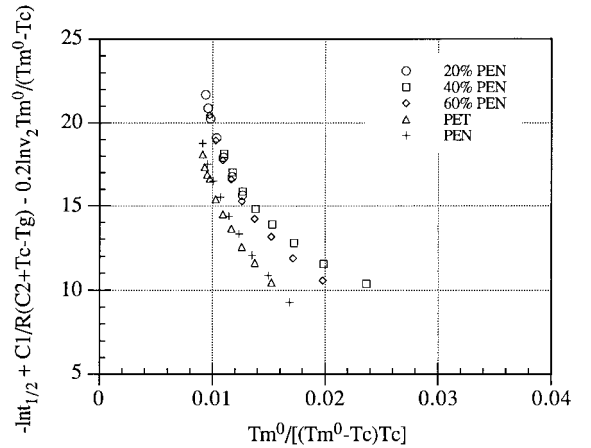$$= A_2 - 4b_0\sigma\sigma_e\frac{T_m}{k\Delta H(T_m - T)T} \quad (17)$$

the straight lines plotted according to eq. (12) and at least $\sigma\sigma_e$ can be obtained. But at this point, additional information is needed for the calculation of $\sigma\sigma_e$. T_m^0 was obtained as described in the previous study,[1] although b_0 and ΔH for the blend samples are not known. Now, if we consider the equation given by Boon[52] and assume that the blend system behaves like a polymer–diluent mixture, then the free energy of the nucleus formation ($\Delta\Phi$) has the form

$$\Delta\Phi = 4b_0\sigma\sigma_e\frac{T_m}{\Delta H(T_m - T)}$$
$$- \frac{2\sigma kT(\ln \varphi_2)T_m}{b_0\Delta H(T_m - T)} \quad \text{(regimes I and III)} \quad (13)$$

$$\Delta\Phi = 2b_0\sigma\sigma_e\frac{T_m}{\Delta H(T_m - T)}$$
$$- \frac{2\sigma kT \ln \varphi_2 T_m}{b_0\Delta H(T_m - T)} \quad \text{(regime II)} \quad (14)$$

where b_0 is the distance between two adjacent fold planes; σ and σ_e are surface free energies of the lateral side and the fold surfaces, respectively; ΔH is the equilibrium heat of fusion per unit volume; and k is the Boltzmann constant. T_m is the equilibrium melting point and φ_2 is the volume fraction of the crystalline component. In eqs. (13) and (14), the second term represents the demixing process of polymer and diluent molecules. The transport term in eq. (6) can be modified following the original development by Hoffman[53] and later by Hsiao and Sauer[35] utilizing the WLF equation. The new term is

Figure 13   Plot of eq. (19) for B blends.

Table V $b_0\sigma\sigma_e$ **for A Blend Samples**

NDC (mol %)	Slope 1 ($\times10^{-2}$)	$b_0\sigma\sigma_e$ (II) ($\times10^{-20}$)	Slope 2 ($\times10^{-2}$)	$b_0\sigma\sigma_e$ (III) ($\times10^{-20}$)	Ratio Slope 2/Slope 1	Transition Temperature (°C)	Supercooling (°C)
0	6.71	65.0	15.7	76.0	2.3	170	106
13.6	7.74	74.9	18.8	91.2	2.4	170	102
31.2	4.17	43.1	11.1	53.9	2.6	170	82
56.3	4.41	45.8	10.6	55.2	2.4	185	84
78.2	8.41	87.3	18.9	98.3	2.2	185	106
100	8.62	91.4	16.1	85.3	1.9	195	111

Regime II

$$-\ln t_{1/2} + \frac{C_1}{R(C_2 + T - T_g)} - 0.2\ln\varphi_2\frac{T_m}{T_m - T}$$

$$= A_2 - 2b_0\sigma\sigma_e\frac{T_m}{k\Delta H(T_m - T)T} \quad (18)$$

All regimes

$$-\ln t_{1/2} + \frac{C_1}{R(C_2 + T - T_g)} - 0.2\ln\varphi_2\frac{T_m}{T_m - T}$$

$$= A_2 - K_g\frac{T_m}{(T_m - T)T} \quad (19)$$

Thus, a plot of the left-hand side of eq. (19) versus $T_m/[(T_m - T)T]$ should give a straight line. The slope of this straight line gives the value of K_g. Volume fraction φ_2 was calculated from the NDC content and the molar volume of the PET and PEN repeat units. Densities of PET and PEN are: ρ_{PET} = 1.333 g/cm^3,[54] ρ_{PEN} = 1.327 g/cm^3.[14] The plot based on eq. (19) is shown in Figures 12 and 13 for both blend systems. The regime transition can be clearly seen in these two plots. The ratio of the slopes of the two straight lines gives values close to 2, which is expected from the the-

ory. The slope of every straight line is listed in Tables V and VI for both blend systems.

The slopes of these straight lines give the value of $-4b_0\sigma\sigma_e/(k\Delta H)$ or $-2b_0\sigma\sigma_e/(k\Delta H)$). Values for $b_0\sigma\sigma_e$ can be obtained using the value of ΔH = 121.3 J/mol for PET[22] and ΔH = 103.3 J/mol for PEN.[22] For further calculations, b_0 must be known. This value can be obtained for pure PET and PEN from the literature, but for the blends or copolymers of PET/PEN, additional experiments must be done using X-ray or small-angle X-ray scattering (SAXS). As a first approximation it was assumed that b_0 is similar for both pure PET and PEN as well as for the various blend compositions, so that the combined value of $b_0\sigma\sigma_e$ provides a relative comparison of the surface free energy. The combined value $b_0\sigma\sigma_e$ was then plotted as a function of the blend composition. The plots are shown in Figures 14 and 15 for both blend systems. Comparing these two plots with plots obtained for the activation energy of rate constant k and the K_g(II) and K_g(III) plots obtained previously, we can easily find that they are similar in appearance. They all pass through a minimum at the intermediate blend composition and jump or decrease from pure PET and PEN values to those of the blends, depending on the

Table VI $b_0\sigma\sigma_e$ **for B Blend Samples**

NDC (mol %)	Slope 1 ($\times10^{-2}$)	$b_0\sigma\sigma_e$ (II) ($\times10^{-20}$)	Slope 2 ($\times10^{-3}$)	$b_0\sigma\sigma_e$ (III) ($\times10^{-20}$)	Ratio Slope 2/Slope 1	Transition Temperature (°C)	Supercooling (°C)
0	9.22	89.2	2.18	105.7	2.4	155	121
17.7	13.6	131.2	2.62	126.7	1.9	150	116
33.3	4.13	40.0	0.99	47.7	2.4	180	76
53.9	7.37	153.0	1.99	183.9	2.7	180	96
100	8.88	92.3	1.83	95.1	2.1	200	107
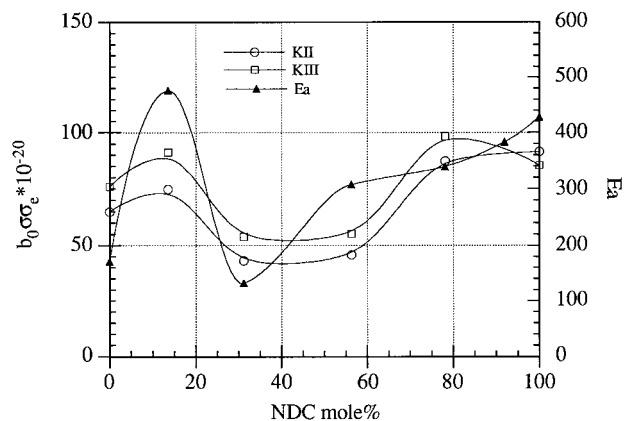
Figure 14 Plot of $b_0\sigma\sigma_e$ versus NDC content for A blends.

Figure 16 Universal plot for PET/PEN blends.

Avrami exponent. Here it is worthwhile to point out that the purpose of making this plot is to see the changing trend. For more accurate values, more experiments should be done. Even such rough assumptions, however, give good agreement with the previous data. Also shown in Tables V and VI are the temperatures at which regime transitions occurred. Using the equilibrium melting points, calculated from the previous study,[1] the degree of supercooling can be calculated from these data. The calculated degrees of supercooling are also listed in the same tables as the regime transitions for both blend systems. The changing trends of degrees of supercooling also follow the same trends as those of K_g and E_a.

Universal Plot

In 1972, in his study of the crystallization of polymers, Gandica[55] found that a universal plot can
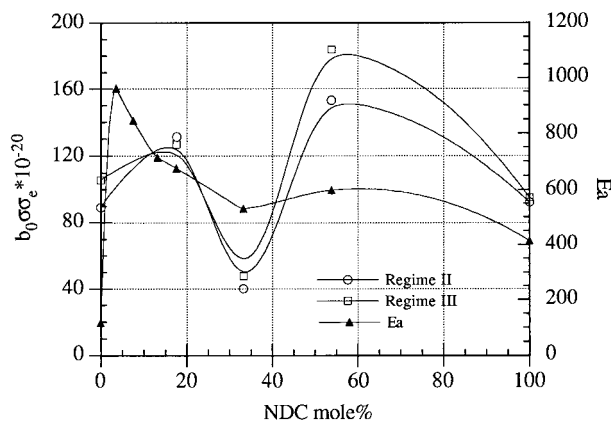

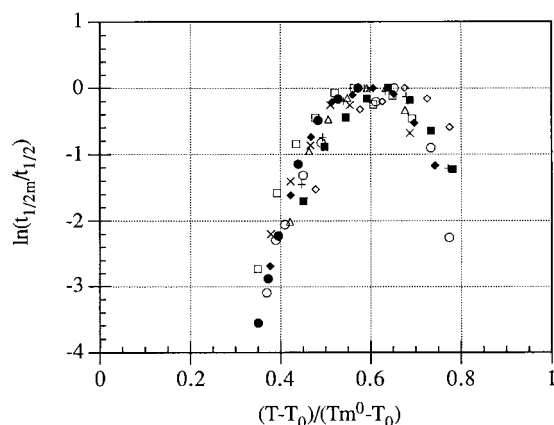**Figure 15** Plot of $b_0\sigma\sigma_e$ versus NDC content for B blends.

be constructed if reduced parameters are used. The idea of Gandica's method can be described using the following equation:

$$\ln\left(\frac{G}{G_x}\right) = f\left(\frac{T - T_0}{T_m - T_0}\right) \qquad (20)$$

Here G is the spherulite growth rate, G_x is the maximum rate of crystallization, T_m is the equilibrium melting point, and T_0 is the temperature predicted by the WLF equation, which is usually 50°C below T_g. By plotting the left-hand side of eq. (20) with respect to $(T - T_0)/(T_m - T_0)$, Gandica found that all the experimental data fell on the same universal curve, or master plot, as he termed it. The curve has a peak at about 0.63 and tends to zero at T_0 and T_m, respectively. Bulk crystallization plots of polymer curves were also examined in a similar manner. It is worthwhile to point out that in constructing this universal plot or master plot, the experimental data he used were from crystallization of different polymers and crystallized from either the glassy state or the melted state.

Using a similar method, we also constructed a universal plot for our blend systems. Here we used the half-time as a measure of the crystallization rate. The $\ln[t_{1/2m}/t_{1/2}]$ was plotted against $(T - T_0)/(T_m - T_0)$ for both blend systems. The $t_{1/2m}$ is the minimum half-time for a given blend composition. The resultant plots are shown in Figure 16. The experimental data here came from blends as well as from pure PET and PEN. The data were also from different blend systems. When plotted using the reduced half-time against the reduced temperature, however, they all fell on the same master curve. A universal plot was thus

constructed for all the samples of the PET/PEN blend systems. This curve has a peak near 0.6. In this manner, the internal consistency of the crystallization data in the blend system was verified. This method also provides a means for extrapolating values from limited available information and should be very useful in the case of actual applications.

CONCLUSIONS

The crystallization kinetics of two different PET/PEN blend systems were investigated. The results lead to the following conclusions.

The crystallization kinetics can be described by the Avrami equation for all the blend samples as well as for pure PET and PEN, within the crystallization temperature range investigated. The Avrami exponent (n) is 4 for all the blend samples. It is 3 for pure PET and is 3 or 4 for pure PEN, depending on the type of PEN used. Different n values indicate different nucleation and crystalline growth processes. For blends, processes are sporadic nucleation; for pure PET, they are instantaneous nucleation. They are either instantaneous or sporadic nucleation for pure PEN, depending on the PEN used. The rate constants (k) are extremely temperature sensitive and can be used to calculate actuation energies of crystallization using an Arrhenius-type expression. The activation energy shows a jump from pure PET, when plotted against blend composition, resulting from different nucleation mechanisms. Instantaneous nucleation gives much lower activation energies than does sporadic nucleation. E_a has a minimum value at the intermediate blend composition because of the formation of less perfect crystalline structures. Regime theory was used to study the crystallization kinetics both of PET/PEN blends and of pure PET and PEN. All blend samples showed transitions from regime II to regime III, as the crystallization temperatures were decreased. The ratio of the slopes of the two straight lines for each sample gives a value close to 2, as expected by regime theory. The nucleation exponent K_g changes with blend composition in a similar way to that of the activation energy, indicating the surface free energy for the formation of nuclei changes with blend composition. It has a minimum value at the intermediate blend composition and is larger for sporadic nucleation than for instantaneous nucleation. A universal plot (master curve) can be constructed by using reduced temperature and reduced half-time or crystallization rate. All experimental data fall on the same master plot for all blend systems.

REFERENCES

1. Shi, Y.; Jabarin, S. A. J Appl Polym Sci 2001, 81, 11.
2. Cobbs, W. H.; Burton, R. L. J Polym Sci 1953, 12, 275.
3. Keller, A.; Lester, G. R.; Morgan, C. B. Philos Trans R Soc London 1954, A247, 1.
4. Hartley, F. D.; Lord, F. W.; Morgan, C. B. Philos Trans R Soc London 1954, A247, 23.
5. Jackson, J. B.; Longman, G. W. Polymer 1969, 10, 873.
6. Van Antwerpen, F.; Van Krevelen, D. W. J Polym Sci Part C 1970, 30, 271.
7. Gunther, B.; Zachmann, H. G. Polymer 1983, 24, 1008.
8. Jabarin, S. A. J Appl Polym Sci 1987, 34, 85.
9. Jabarin, S. A. J Appl Polym Sci 1987, 34, 97.
10. Jabarin, S. A. J Appl Polym Sci 1987, 34, 103.
11. Cheng, S. Z. D.; Wunderlich, B. Macromolecules 1988, 21, 789.
12. Medellin-Rodriguez, F. J.; Phillips, P. J. ANTEC 1991, 37, 893.
13. Zachmann, H. G.; Wiswe, D.; Gehrke, R.; Riekel, C. Makromol Chem Suppl 1985, 12, 175.
14. Buchner, S.; Wiswe, D.; Zachmann, H. G. Polymer 1989, 30, 480.
15. Medellin-Rodriguez, F. J.; Phillips, P. J.; Lin, J. S. Macromolecules 1996, 26, 7491.
16. Menick, Z. Chem Prim 1967, 17, 78.
17. Heisey, C. L.; Hoffman, D. C.; Zawada, J. A. Polym Prepr 1996, 231.
18. Po, R.; Occhiello, E.; Giannotta, G.; Luigi, P.; Abis, L. Polym Adv Technol 1996, 7, 365.
19. Lu, X.; Windle, A. H. Polymer 1995, 36, 451.
20. Stewart, M. E.; Cox, A. J.; Taylor, D. M. Polymer 1993, 34, 4060.
21. Callunder, D.; Sisson, E. in Bev-Pak, Americas 1994.
22. McGee, T. M.; Jones, A. S. in The Effect of Processing Parameters on Physical Properties of PET/PEN Blends for Bottle Applications, SPE 11th Annual High Performance Blow Molding Presentation, Cleveland, Ohio, October 1995; pp. 91–106.
23. Jenkins, S. D. in Proceedings of Specialty Polyesters '95 Conference, Munich, 1995; p. 197.
24. Santa Cruz, C.; Balta Calleja, F. J.; Zachmann, H. G.; Chen, D. J Mater Sci 1992, 27, 2161.
25. Hoffman, D. C.; Caldwell, J. K. in Proceedings of Specialty Polyesters '95 Conference, Munich, 1995.

26. Ihm, D. W.; Park, S. Y.; Chang, C. G.; Kim, Y. S.; Lee, H. K. J Polym Sci Part A Poly Chem 1996, 34, 2841.

27. Shi, Y. Ph.D. Dissertation, Polymer Institute, The University of Toledo, 1998.

28. Hoffman, J. D.; Davis, G. T.; Lauritzen, J. I., Jr. Treatise on Solid State Chemistry; Hannay, N. B., Ed.; Plenum Press: New York, 1976; Vol. 3, Chapter 7.

29. Hoffman, J. D. Polymer 1983, 24, 3.

30. Hoffman, J. D.; Frolen, L. J.; Ross, G. S.; Lauritzen, J. I., Jr. J Res Natl Bur Stand 1975, A79, 671.

31. Vasanthakumari, R.; Pennings, A. J. Polymer 1983, 24, 175.

32. Pelzbauer, Z.; Galeske, A. J Polym Sci Part C 1972, 38, 23.

33. Clark, E. J.; Hoffman, J. D. Macromolecules 1984, 17, 878.

34. Mandelkern, L. J Appl Phys 1955, 26, 443.

35. Hsiao, B. S.; Sauer, B. B. J Polym Sci Part B Polym Phys 1993, 31, 901.

36. Booth, A.; Hay, J. N. Polymer 1969, 10, 95.

37. Hay, J. N.; Sabir, M. Polymer 1969, 10, 203.

38. Fielding-Russell, G. S.; Pillai, P. S. Makromol Chem 1970, 135, 263.

39. Mandelkern, L. Crystallization of Polymers; McGraw-Hill: New York, 1964.

40. Sharples, A. Introduction to Polymer Crystallization; Edward Arnold: London, 1966.

41. Meares, P. Polymers: Structure and Bulk Properties; Van Nostrand: London, 1965.

42. Shi, Y.; Jabarin, S. A. J Appl Polym Sci 2000, 80, 2422.

43. Wunderlich, B. Macromolecular Physics: Crystal Melting, Vol. 3; Academic: New York, 1980.

44. Smith, J. M. Chemical Engineering Kinetics; McGraw-Hill: New York, 1981.

45. Flory, P. J. J Chem Phys 1949, 17, 223.

46. Flory, P. J.; Vrij, A. J Am Chem Soc 1963, 85, 3548.

47. Wunderlich, B.; Czornyj, G. Macromolecules 1977, 10, 960.

48. Hoffman, J. D. Polymer 1982, 23, 656.

49. Supaphol, P. H.; Wu, J. J.; Phillips, P. J.; Spruiell, J. E. ANTEC 1997, 387, 1759.

50. Guttman, C. M.; DiMaezio, E. A. J Appl Phys 1983, 54, 5541.

51. Stack, G. M. Ph.D. Dissertation, Florida State University, 1983.

52. Boon, J.; Azcure, J. M. J Polym Sci 1968, A2, 885.

53. Hoffman, J. D. SPE Trans 1964, 315.

54. Jabarin, S. A. PET Technology Seminar, University of Toledo, 1996.

55. Gandica, A.; Magill, J. H. Polymer 1972, 13, 595.